Inorg. Chem. **2004**, *43*, 5003–5010

Application of a Universal Force Field to Mixed Fe/Mo–S/Se Cubane and Heterocubane Clusters. 1. Substitution of Sulfur by Selenium in the Series $[Fe_4X_4(YCH_3)_4]^{2-}$; X = S/Se and Y = S/Se†

Axel Kern, Christian Näther, Felix Studt, and Felix Tuczek*

Institut für Anorganische Chemie, Christian Albrechts Universität Kiel, D-24098 Kiel, Germany

Received December 29, 2003

A series of Fe–S and Fe–Se cubane clusters containing all four combinations of the general formula $[Fe_4X_4(Y–CH_3)_4]^{2-}$ (X = S/Se, Y = S/Se) is investigated with FTIR and Raman spectroscopy. The terminally selenolate coordinated clusters (Y = Se) are prepared by a new synthetic route. All four cluster compounds are structurally characterized by X-ray single-crystal structure determination. Infrared and Raman spectra of all compounds are presented and interpreted with normal coordinate analysis. The corresponding force fields are based on that developed for the Fe_4S_4–benzyl cluster (Czernuszewicz, R. S.; Macor, K. A.; Johnson, M. K.; Gewirth, A.; Spiro, T. G. *J. Am. Chem. Soc.* **1987**, *109*, 7178–7187). An empirical procedure is presented to convert Fe–S into Fe–Se force constants. Only minor changes in force constants are found upon S → Se exchange, reflecting the similarity of the Fe–S and Fe–Se bonds. The drastic frequency shifts in the metal–ligand region observed upon substitution of sulfur by selenium are, therefore, primarily due to the corresponding mass changes.

I. Introduction

Iron sulfur proteins are ubiquitous enzymes which are involved in a variety of biological functions.[1] Most of them contain iron sulfur clusters (Fe_2S_2, Fe_3S_4, Fe_4S_4) at their active sites. Mixed iron/heterometal sulfur clusters are much less abundant. A prominent example for this class of active sites is the iron−molybdenum cofactor (FeMoco) of the enzyme nitrogenase, which mediates biological nitrogen fixation.[2] On the basis of protein crystallography, the FeMoco is composed of two cubane clusters, Fe_4S_3X and $MoFe_3S_3X$, which are connected via their common X atom and three additional sulfido bridges (X = N, O, or C).[3] According to current knowledge, the FeMoco is the reactive center of nitrogenase, where N_2 is bound and reduced to NH_3. Analogous clusters are present in the P-cluster of nitrogenase and in the FeVaco/FeFeco of alternative (vanadium or iron-only) nitrogenases, where the molybdenum atom of the FeMoco is replaced by V and Fe, respectively.[3e,4] Corresponding synthetic clusters have become available recently.[5]

An important experimental technique in the study of biological iron−sulfur centers is Raman spectroscopy.[6] By direct spectroscopic comparison with corresponding small-molecule model systems coupled with normal coordinate analysis, electronic and geometric structures of many Fe_2S_2,

* To whom correspondence should be addressed. E-mail: ftuczek@ac.uni-kiel.de.

† Dedicated to Philipp Gütlich on the occasion of his 70th birthday.

(1) (a) Beinert, H.; Holm, R. H.; Münck, E. *Science* **1997**, *277*, 653−659. (b) Beinert, H. *J. Biol. Inorg. Chem.* **2000**, *5*, 2−15. (c) Johnson, M. K.; Duderstadt, R. E.; Duin, E. C. In *Advances in Inorganic Chemistry*; Cammack, R., Sykes, A. G., Eds.; Academic Press: San Diego, 1999; Vol. 47, pp 1−82. (d) Holm, R. H.; Kennepohl, P.; Solomon, E. I. *Chem. Rev.* **1996**, *96*, 2239−2314. (e) Holm, R. H. In *Advances in Inorganic Chemistry*; Cammack, R., Sykes, A. G., Eds.; Academic Press: San Diego, 1992; Vol. 38, pp 1−71. (f) *Iron Sulfur Proteins*; Spiro, T. G., Ed.; Wiley Interscience: New York, 1982.

(2) *Prokaryotic Nitrogen Fixation: A Model System for the Analysis of a Biological Process*; Triplett, E. W., Ed.; Horizon Scientific Press: Wymondham, U.K., 2000.

(3) (a) Einsle, O.; Tezcan, F. A.; Andrade, S. L. A.; Schmid, B.; Yoshida, M.; Howard, J. B.; Rees, D. C. *Science* **2002**, *297*, 1696−1700 and references. cited therein. (b) Lee, H.-I.; Benton, P. M. C.; Laryukhin, M.; Igarashi, R. Y.; Dean, D. R.; Seefeldt, L. C.; Hoffman, B. M. *J. Am. Chem. Soc.* **2003**, *125*, 5604−5605. (c) Smith, B. E. In *Advances in Inorganic Chemistry*; Cammack, R., Sykes, A. G., Eds.; Academic Press: San Diego, 1999; Vol. 47, pp 159−218. (d) Schindelin, H.; Kisker, C.; Schlessman, J. L.; Howard, J. B.; Rees, D. C. *Nature* **1997**, *387*, 370−376. (e) Eady, R. R. *Chem. Rev.* **1996**, *96*, 3013−3030. (f) Lee, H.-I.; Benton, P. M. C.; Laryukhin, M.; Igarashi, R. Y.; Dean, D. R.; Seefeldt, L. C.; Hoffman, B. M. *J. Am. Chem. Soc.* **2003**, *125*, 5604−5605.

(4) (a) Krahn, E.; Weiss, B. J. R.; Knöchel, M.; Groppe, J.; Henkel, G.; Cramer, S. P.; Trautwein, A. X.; Schneider, K.; Müller, A. *J. Biol. Inorg. Chem.* **2002**, *7*, 37. (b) Krahn, E.; Schneider, K.; Müller, A. *Appl. Microbiol. Biotechnol.* **1996**, *46*, 285.

(5) (a) Zhang, Y.; Holm, R. H. *J. Am. Chem. Soc.* **2003**, *125*, 3910−3920. (b) Zhang, Y.; Zuo, J.-L.; Zhou, H.-C.; Holm, R. H. *J. Am. Chem. Soc.* **2002**, *124*, 14292−14293. (c) Zuo, J.-L.; Zhou, H.-C.; Holm, R. H. *Inorg. Chem.* **2003**, *42*, 4624−4631. (d) Ohki, Y.; Sunada, Y.; Honda, M.; Katada, M.; Tatsumi, K. *J. Am. Chem. Soc.* **2003**, *125*, 4052−4053. (e) Coucouvanis, D.; Han, J.; Moon, N. *J. Am. Chem. Soc.* **2002**, *124*, 216−224. (f) Han, J.; Coucouvanis, D. *Inorg. Chem.* **2002**, *41*, 2738−2746.

10.1021/ic030347d CCC: $27.50
Published on Web 07/09/2004

Fe_3S_4, and Fe_4S_4 clusters present in iron−sulfur proteins were determined. In an effort to characterize iron−sulfur clusters with relevance to the FeMoco using Raman spectroscopy, we started a program to investigate the Raman and IR spectra of $MoFe_3S_4$ cubane clusters and compare them to those of their Fe_4S_4 counterparts. One potential experimental problem encountered with these systems is Raman intensity deenhancement caused by overlapping charge-transfer bands.[7] This phenomenon is relevant in the case of metal−sulfur clusters, as the UV−vis spectra of these molecules have many closely spaced CT transitions in the visible/near-UV region.[8] Apart from looking for a possible change of Raman intensities associated with the Fe → Mo substitution, we were also interested in the relationship between the vibrational spectra of MoFe clusters and those of their iron-only counterparts. For the Fe_4S_4−benzyl cluster $[Fe_4S_4(S-CH_2-Ph)_4]^{2-}$ ("benzyl cube"), a force field has been developed.[9] We specifically wanted to determine whether suitable adaptation of this force field would also describe the vibrational frequencies of $MoFe_3S_4$ clusters.

To obtain further information on the generality of the force field of the benzyl cluster, it was also of interest to vary the nonmetallic component of Fe_4S_4 cubane clusters through replacement of sulfur by selenium. It has been questioned whether S → Se substitution would be of use in the elucidation of the vibrational structure of iron−sulfur clusters, as the doubling of the bridging atom masses might alter the mode compositions and thus make correlations difficult.[6e] Although spectroscopic Raman investigations on Fe_4Se_4 clusters exist,[10] no systematic investigation of this problem has been performed. Selenolate coordinated clusters are known as well,[11] but to our knowledge have not been structurally characterized. Moreover, the spectroscopic consequences of an exchange of the terminal thiolate ligands by terminal selenolate ligands have not been studied for Fe_4S_4 clusters. The first part of the present study therefore presents vibrational studies on a homologous series of four Fe−S/Se clusters, $[Fe_4X_4(Y-CH_3)_4]^{2-}$, X = Y = S (**1**), X = Se and Y = S (**2**), X = S and Y = Se (**3**), and X = Y = Se (**4**), all of which are structurally characterized. To carry the structural analogy as far as possible, identical organic residues (R = CH_3) and counterions (tetrabutylammonium, TBA) were chosen. The thiolate coordinated clusters were prepared according to a literature procedure.[12] For the synthesis of the selenolate coordinated Fe_4S_4 and Fe_4Se_4 clusters, a new synthetic route has been developed; i.e., we found that these systems can be prepared by conversion of the easily accessible halide coordinated clusters $[Fe_4X_4Hal_4]^{2-}$ (X = S/Se; Hal = Cl, Br[13]) with the corresponding diselenides in the presence of tetra-*n*-butylammonium borohydride and triethylamine. On the basis of the force field of the benzyl cluster, the spectra of all clusters are analyzed, applying an empirical procedure for the first guess of the respective force fields.

The second part of the present study (part 2, accompanying paper) describes analogous investigations on $MoFe_3S_4$ clusters with terminal thiolate and halide ligands, with vibrational analysis again resting on the force field of the benzyl cube. First, the spectra of $Fe_4(S/Se)_4$ clusters with terminal halides are presented and analyzed. Then, $MoFe_3S_4$ clusters with terminal thiolates are considered, correlating the results to those obtained on the corresponding Fe_4S_4 systems in this part of the study. Finally, the spectra of $MoFe_3S_4$ clusters with terminal halide ligands are analyzed and compared to those of their all-iron counterparts, i.e., Fe_4S_4 cubane clusters with chloro, bromo, and iodo ligands. General implications of the results are discussed.

II. Experimental Section

All reactions were performed using Schlenk techniques on a vacuum/inert gas line (Argon 4.6). Compounds were handled and samples for spectroscopy prepared in gloveboxes (M. Braun, Labmaster 130) in an argon atmosphere. $(TBA)_2[Fe_4S_4(S-CH_3)_4]$ (**1**) and $(TBA)_2[Fe_4Se_4(S-CH_3)_4]$ (**2**) were prepared from $FeCl_2$, $NaSCH_3$, and elemental sulfur (**1**) and selenium (**2**), respectively, employing a literature procedure.[12] $(TBA)_2[Fe_4S_4(Se-CH_3)_4]$ (**3**) was prepared as follows: $(n\text{-}Bu_4N)_2[Fe_4S_4Cl_4]$[13] (0.36 g, 0.37 mmol) was dissolved in 40 mL of CH_3CN. To a solution of 0.41 g (1.6 mmol) of $(n\text{-}Bu_4N)BH_4$ in 40 mL of CH_3CN was added 0.14 g (0.74 mmol) of dimethyl diselenide in 20 mL of CH_3CN. The borohydride/diselenide mixture was then added to the cluster

(6) (a) Spiro, T. G.; Czernuszewicz, R. S.; Han, S. *Biological Applications of Raman Spectroscopy*; Spiro, T. G., Ed.; John Wiley & Sons: New York, 1988; Chapter 12. (b) Czernuszewicz, R. S.; Kilpatrick, L. K.; Koch, S. A.; Spiro, T. G. *J. Am. Chem. Soc.* **1994**, *116*, 7134−7141. (c) Kilpatrick, L. K.; Kennedy, M. C.; Beinert, H.; Czernuszewicz, R. S.; Qiu, D.; Spiro, T. G. *J. Am. Chem. Soc.* **1994**, *116*, 4053−4061. (d) Han, S.; Czernuszewicz, R. S.; Kimura, T.; Adams, M. W. W.; Spiro, T. G. *J. Am. Chem. Soc.* **1989**, *111*, 3504−3511. (e) Han, S.; Czernuszewicz, R. S.; Spiro, T. G. *J. Am. Chem. Soc.* **1989**, *111*, 3496−3505. (f) Yachandra, K. V.; Hare, J.; Gewirth, A.; Czernuszewicz, R. S.; Kimura, T.; Holm, R. H.; Spiro, T. G. *J. Am. Chem. Soc.* **1983**, *105*, 6462−6468. (g) Yachandra, K. V.; Hare, J.; Moura, I.; Spiro, T. G. *J. Am. Chem. Soc.* **1983**, *105*, 6455−6461. (h) Backes, G.; Mino, Y.; Loehr, T. M.; Meyer, T. E.; Cusanovich, M. A.; Sweeney, W. V.; Adman, E. T.; Sanders-Loehr, J. *J. Am. Chem. Soc.* **1991**, *113*, 2055−2064. (i) Agar, J. N.; Zheng, L.; Cash, V. L.; Dean, D. R.; Johnson, M. K. *J. Am. Chem. Soc.* **2000**, *122*, 2136−2137.

(7) Spiro, T. G.; Stein, P. *Annu. Rev. Phys. Chem.* **1977**, *28*, 501−521.

(8) (a) Aizman, A.; Case, D. A. *J. Am. Chem. Soc.* **1982**, *104*, 3269−3279. (b) Noodleman, L.; Norman, J. G.; Osborne, J. H.; Aizman, A.; Case, D. A. *J. Am. Chem. Soc.* **1985**, *107*, 3418−3426

(9) Czernuszewicz, R. S.; Macor, K. A.; Johnson, M. K.; Gewirth, A.; Spiro, T. G. *J. Am. Chem. Soc.* **1987**, *109*, 7178−7187.

(10) (a) Meyer, J.; Moulis, J.-M.; Gaillard, J.; Lutz, M. In *Advances in Inorganic Chemistry*; Cammack, R., Sykes, A. G., Eds.; Academic Press: San Diego, 1992; Vol. 38, pp 73−115. (b) Moulis, J.-M.; Lutz, M.; Gaillard, J.; Noodleman, L. *Biochemistry* **1988**, *27*, 8712−8719. (c) Moulis, J.-M.; Meyer, J.; Lutz, M. *Biochemistry* **1984**, *23*, 6605−6613. (d) Beardwood, P.; Gibson, J. G. *J. Chem. Soc., Dalton Trans.* **1984**, 1507−1516.

(11) (a) Bobrick, M. A.; Laskowski, E. J.; Johnson, R. W.; Gillum, W. O.; Berg, J. M.; Hodgson, K. O.; Holm, R. H. *Inorg. Chem.* **1978**, *17*, 1402−1410. (b) Yu, S.-B.; Papaefthymiou, G. C.; Holm, R. H. *Inorg. Chem.* **1991**, *30*, 3476−3485 and references cited therein. (c) Nakamoto, M.; Fukaishi, K.; Tagata, T.; Kambayashi, H.; Tanaka, K. *Bull. Chem. Soc. Jpn.* **1999**, *72*, 407−414. (d) Nakamoto, M.; Tanaka, K.; Tanaka, T. *Bull. Chem. Soc. Jpn.* **1988**, *61*, 4099−4105.

(12) Christou, G.; Garner, C. D. *J. Chem. Soc., Dalton Trans.* **1979**, 1093−1094.

(13) Details on the synthesis of iron sulfur and selenium clusters with halide ligands are given in the following paper. (a) Ahle, A.; Dehnicke, K.; Maichle-Mossmer, C.; Strähle, J. *Z. Naturforsch.* **1994**, *49B*, 434−436. (b) Müller, A.; Schladerbeck, N. H.; Bögge, H.; Schmitz, K. *Z. Anorg. Allg. Chem.* **1989**, *570*, 7−36. (c) Rutchik, S.; Kim, S.; Walters, M. A. *Inorg. Chem.* **1988**, *27*, 1513−1516. (d) Bobrick, M. A.; Hodgson, K. O.; Holm, R. H. *Inorg. Chem.* **1977**, *16*, 1851−1858. (e) Wong, G. B.; Bobrick, M. A.; Holm, R. H. *Inorg. Chem.* **1978**, *17*, 578−584.

Table 1. Crystal Data and Results of the Structure Refinement for Compounds **1**−**4**[a]

	1	**2**	**3**	**4**
chemical formula	$[Fe_4S_4(CH_3S)_4](TBA)_2$	$[Fe_4Se_4(CH_3S)_4](TBA)_2$	$[Fe_4S_4(CH_3Se)_4](TBA)_2$	$[Fe_4Se_4(CH_3Se)_4](TBA)_2$
fw	1024.93	1212.53	1212.53	1400.13
T	150 K	150 K	150 K	150 K
λ	0.71073 Å	0.71073 Å	0.71073 Å	0.71073 Å
cryst syst	orthorhombic	orthorhombic	orthorhombic	orthorhombic
space group	*Pba*2	*Pba*2	*Pba*2	*Pba*2
a	15.941(1) Å	16.136(1) Å	16.052(1) Å	16.209(1) Å
b	17.094(1) Å	17.292(2) Å	17.435(1) Å	15.575(1) Å
c	9.4825(6) Å	9.3465(6) Å	9.4972(5) Å	9.3752(4) Å
V	2584.0(3) Å^3	2607.9(3) Å^3	2658.0(3) Å^3	2670.8(3) Å^3
Z	2	2	2	2
D_{calcd}	1.317 g cm^{-3}	1.544 g cm^{-3}	1.515 g cm^{-3}	1.741 g cm^{-3}
μ	1.45 cm^{-1}	4.07 cm^{-1}	3.99 cm^{-1}	6.54 cm^{-1}
R_1 [$I > 2\sigma(I)$]	0.0307	0.0414	0.0294	0.0297
wR_2 [all data]	0.0721	0.1075	0.0750	0.0777

[a] $R_1 = \sum||F_o| - |F_c||/\sum|F_o|$; $wR_2 = [\sum[w(F_o^2 - F_c^2)^2]/\sum[w(F_o^2)^2]]^{1/2}$.

Table 2. Geometry Parameters of Clusters **1**−**4** Adapted to D_{2d} Symmetry[a]

compd	r^{b1}	r^{b2}	r^t	α^{xy}	α^z	β^{xy}	β^z	γ^{xy}	γ^z	b^{xy}	b^z	a^{xy}	a^z	c^{xy}	c^z	r^{Y-C}	δ	d
benzyl	2.239	2.310	2.251	104.2	104.0	73.9	73.8	114.1	115.2	2.776	2.732	3.645	3.586	3.827	3.790	1.830	103.8	3.222
1, S^b/S^t	2.268	2.303	2.257	103.2	104.7	74.3	73.3	115.5	112.0	2.781	2.729	3.609	3.620	3.856	3.750	1.815	102.8	3.194
2, Se^b/S^t	2.440	2.399	2.259	104.6	107.4	71.4	70.0	115.0	107.1	2.800	2.777	3.795	3.900	3.929	3.781	1.832	102.1	3.193
3, S^b/Se^t	2.279	2.297	2.381	103.6	105.0	73.8	73.0	115.7	110.8	2.759	2.721	3.609	3.630	3.961	3.836	1.960	99.8	3.332
4, Se^b/Se^t	2.434	2.391	2.375	105.1	107.4	71.0	70.0	115.0	106.6	2.778	2.766	3.795	3.888	4.020	3.856	1.962	99.1	3.311

[a] Designations refer to Figure 3.

solution with a syringe. After addition of 0.3 mL (2.2 mmol) of triethylamine, a reddish color change occurred, and a black solid precipitated. The reaction mixture was stirred overnight. The precipitate was separated by vacuum filtration, washed with 2-propanol, and dried in vacuo. $(TBA)_2[Fe_4Se_4(Se-CH_3)_4]$ (**4**) was prepared as follows: $(n\text{-}Bu_4N)_2[Fe_4Se_4Cl_4]$[13] (0.4 g, 0.34 mmol) was dissolved in 40 mL of CH_3CN. To a solution of 0.41 g (1.6 mmol) of $(n\text{-}Bu_4N)BH_4$ in 40 mL of CH_3CN was added 0.14 g (0.74 mmol) of dimethyl diselenide in 20 mL of CH_3CN. The borohydride/diselenide mixture was added to the cluster solution via a syringe, followed by addition of 0.3 mL (2.2 mmol) of triethylamine. The color of the solution first turned to reddish, and then a black solid precipitated. The reaction mixture was stirred at 45 °C overnight. To completely separate the product, 20 mL of 2-propanol was added, and then the whole mixture was put into the deep freezer (−30 °C) for several hours. The solid exhibiting a black luster was separated by vacuum filtration, washed with 2-propanol, and dried in vacuo. Crystals of **1** which are suitable for X-ray structure analysis were obtained by recrystallization of **1** in CH_3CN. To obtain single crystals of **2**−**4**, a small quantity of cluster compound was dissolved in DMSO and covered with a layer of methanol. The mixture was left for 3 days at room temperature and then slowly cooled to −20 °C. The crystals grew in quadratic plates.

X-ray structure determinations were performed using a STOE IPDS diffractometer. For all compounds, a numerical absorption correction was applied. All structures were solved with direct methods using SHELXS-97 and were refined against F^2 using SHELXL-97. All non-H atoms were refined anisotropically. The H-atoms were positioned with idealized geometry and refined using the riding model. The absolute structures of all compounds were determined and are in agreement with the selected setting [Flack *x*-parameter: 0.00(1) (**1**); 0.00(1) (**2**); 0.002(1) (**3**); 0.00(1) (**4**)]. In addition, refinement of the inverse structures leads to significantly poorer reliability factors. Details of the structure determination are given in Table 1. Lists of bond lengths and angles are given in the Supporting Information. Relevant structural information is given in the following text.

Raman spectra were recorded on a commercial spectrometer (DILOR XY) equipped with a triple monochromator and a CCD camera (ISA Spectrum One). Excitation source was a 2018 Ar^+/Kr^+ mixed gas laser from Spectra Physics. All samples were measured as KBr and RbI pellets, respectively, employing laser powers of 15−25 mW and a spectral resolution of 1.5 cm^{-1}. Sample temperature was kept at 20 K. Infrared spectra were recorded on a Bruker IFS 66 FTIR spectrometer equipped with a CTI cryocooler. The sample temperature was set at 20 K. Normal coordinate analyses were performed with the program MOLVIB.[14]

III. Results and Analysis

A. Structural Correlations. The present series of homologous $Fe_4(S/Se)_4$ clusters provides the opportunity to study the structural, electronic, and vibrational properties of cubane clusters in a similar crystalline matrix. All compounds **1**−**4** are isotypic and crystallize in the orthorhombic noncentrosymmetric space group *Pba*2 with 2 formula units in the unit cell (Table 1). The structures consist of $Fe_4(S/Se)_4$ clusters in special positions and tetrabutylammonium cations in general positions. The $Fe_4(S/Se)_4$ clusters are well separated by the organic cations, forming stacks in the direction of the *c*-axis (Figure 1). Each cluster anion is surrounded by 4 tetrabutylammonium cations within the *ab*-plane. All clusters can be described by two interpenetrating Fe_4 and $(S/Se)_4$ tetrahedra and thus possess approximate T_d symmetry (Figure 2). The iron atoms are terminally coordinated by thiolates (Y = S; **1** and **2**) or selenolates (Y = Se; **3** and **4**), with the S and Se atoms, respectively, again forming the vertices of a tetrahedron.

Closer inspection of the molecular structures reveals that all compounds exhibit a distortion of the cluster core that is

(14) (a) Sundius, T. QCPE No. 604, MOLVIB; Indiana University: Indiana 1991. Modified: Bublitz, D. Ph.D. Dissertation, Universität Kiel, 1995. (b) Sundius, T. *J. Mol. Struct.* **1990**, *218*, 321−326. (c) Sundius, T. *Commentat. Phys.−Math.* **1977**, *47*, 1−66.

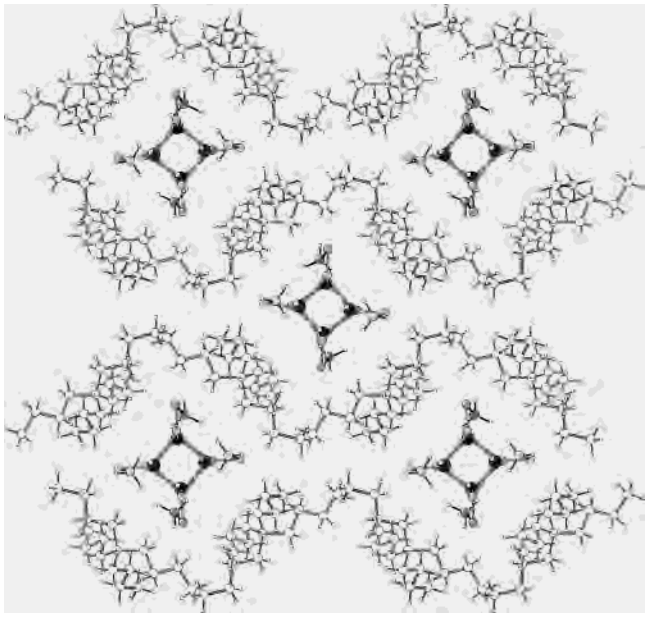

Figure 1. Crystal structure of compounds **1**−**4** with the view in the direction of the crystallographic *c*-axis.

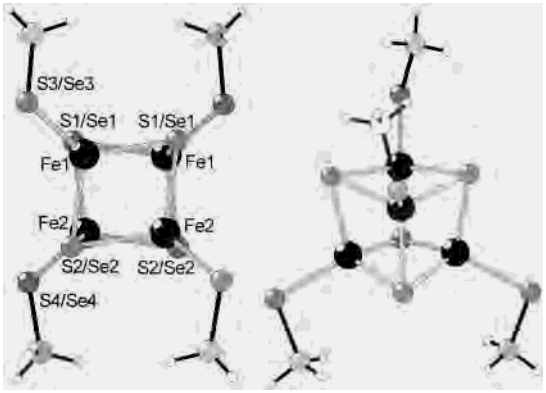

Figure 2. Crystal structure of the Fe_4X_4 clusters for compounds **1**−**4**.

characterized by an elongation of the $(S/Se)_4$ tetrahedron and a compression of the Fe_4 tetrahedron along the *z*-axis. This lowers the symmetry of the cluster core to D_{2d} and generates two sets of Fe−X^b bond distances (X = S/Se; b = bridging), r^{b1} along the *z*-axis and r^{b2} in the *xy*-plane (Figure 3, Table 2). The resulting distortion of the Fe_4X_4 unit (elongation or compression) depends on whether the elongation of the $(S/Se)_4$ tetrahedron (a^z/a^{xy}) is larger than the compression of the Fe_4 tetrahedron (b^z/b^{xy}) or vice versa (Scheme 1). In the first case, the Fe_4X_4 core is elongated ($r^{b1} > r^{b2}$), which is observed for the clusters in compounds **2** and **4** containing Se in the core. In the second case, the Fe_4X_4 unit is compressed ($r^{b1} < r^{b2}$), which applies to the Fe_4S_4 clusters present in compounds **1** and **3**. D_{2d} is also the approximate symmetry of the entire cluster molecule, including the terminal Y−CH_3 groups. Remarkably, the terminal methyl groups in all compounds point into the *z*-direction, orienting the lone pair of the Y-donor atoms along the X−X axis of the respective Fe_2X_2 bent diamond unit. Discussion on the relationship between this configuration and the structural distortions of the cluster core will follow.

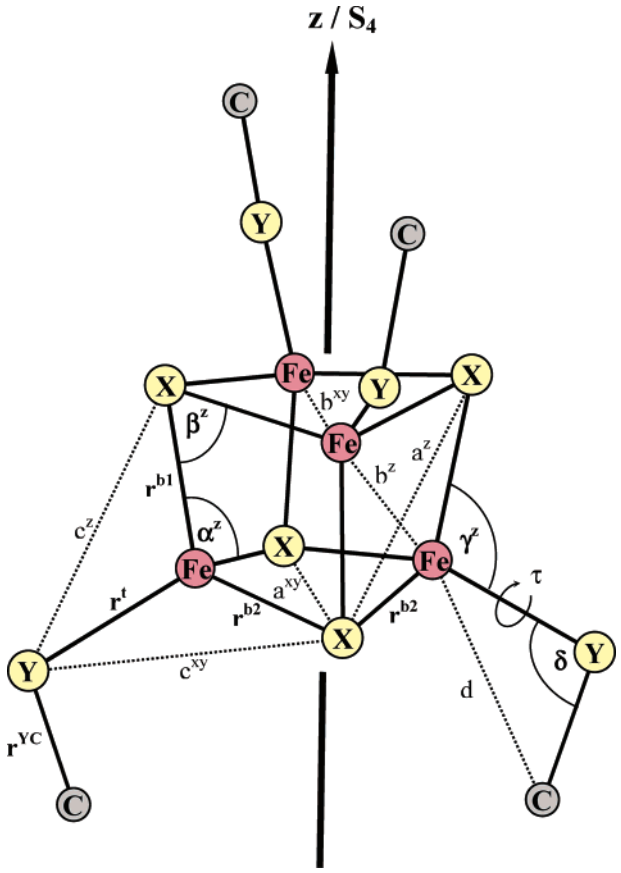

Figure 3. Model of a $[Fe_4X_4(Y-C)_4]$-unit in ideal D_{2d} symmetry with definitions of internal coordinates (bond distances and angles). Coordinates along the *z*-axis are indicated z; coordinates primarily in the *xy*-plane are indicated as xy. Bending coordinates in the *xy*-plane are omitted for clarity.

B. Vibrational Spectroscopy and Normal Coordinate Analysis. The IR and Raman spectra of the four compounds **1**−**4** are given for the range between 140 and 420 cm^{-1} in Figure 4. The 16 stretching vibrations of the $[FeX_4Y_4]$ unit (X = S/Se, Y = S/Se) are observed in this region. They can be divided into four terminal (t) modes Fe−Y and 12 modes involving the bridging (b) ligands X. In tetrahedral symmetry (point group T_d), the t-modes transform according to

$$\Gamma^t_{Fe-Y} = A^t_1 + T^t_2 \quad (1)$$

(designated as I (A^t_1) and II (T^t_2) in Figure 4), and the b-modes correspond to

$$\Gamma^b_{Fe-X} = A^b_1 + E^b + T^b_1 + 2T^b_2 \quad (2)$$

(designated as III (T^b_2), IV (A^b_1), V (E^b), VI (T^b_1), and VII (T^b_2) in Figure 4). The distortion along the *z*-axis corresponds to a lowering of the symmetry to D_{2d} (vide supra) and causes a splitting of the E- and T-modes according to E → $A_1 + B_1$ (Va + Vb), T_1 → $A_2 + E$ (VIa + VIb), and T_2 → $B_2 + E$ (IIa + IIb, IIIa + IIIb, and VIIa + VIIb). According to the selection rules of the parent point group T_d, the IR spectra are dominated by vibrations of T_2 symmetry (II, III, and VII), whereas the Raman spectra in the case of resonance enhancement contain peaks of all symmetries.[9]

Scheme 1

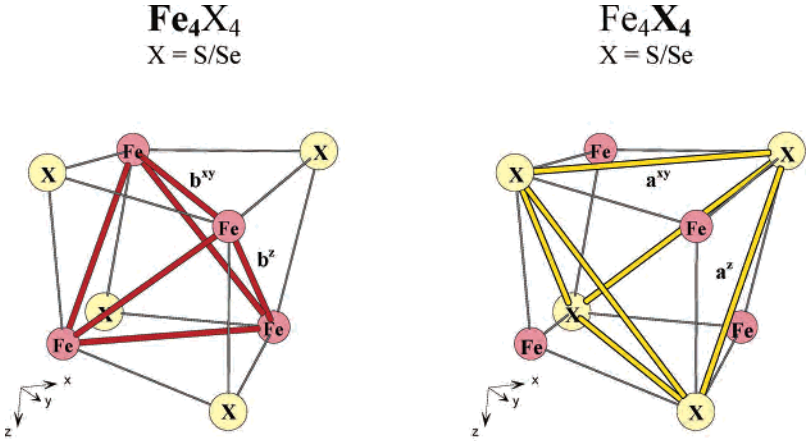

	r^{b1}/r^{b2}	b^z/b^{xy}	a^z/a^{xy}
Benzyl	0.969	0.984	0.984
S^b/S^t	0.985	0.981	1.003
Se^b/S^t	1.017	0.992	1.028
S^b/Se^t	0.992	0.986	1.006
Se^b/Se^t	1.018	0.996	1.025

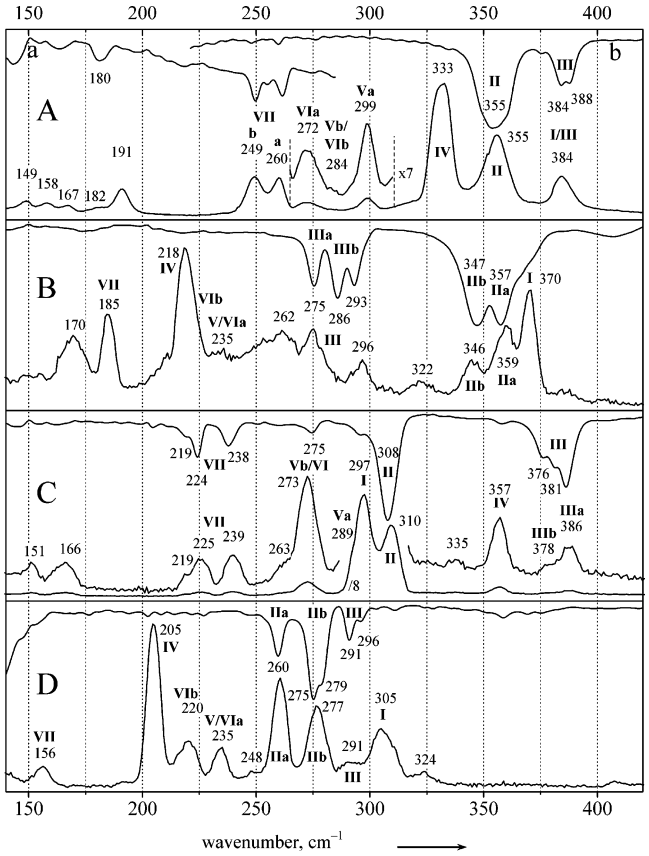

Figure 4. IR and resonance Raman spectra of compounds **1** (A), **2** (B), **3** (C), and **4** (D); upper trace is IR, lower trace is Raman, respectively. Excitation wavelength $\lambda_{exc} = 514.5$ nm, $T = 20$ K. All IR spectra were measured in PE at 20 K (with the exception of Aa, which has been measured at higher concentration than Ab in RbI).

For the benzyl thiolate coordinated cluster $[Fe_4S_4(S-CH_2-Ph)_4]^{2-}$ (benzyl cube), all stretching modes have been assigned in D_{2d} symmetry, employing normal coordinate analysis and ^{34}S isotope substitution.[9] On the basis of a Urey–Bradley force field, which accounts for nonbonding interactions between iron atoms on one hand (Fe–Fe) and sulfur atoms on the other hand (S^b-S^b, S^b-S^t), the experimentally determined frequencies could be reproduced within a couple of wavenumbers. We have augmented this force field by the S–C and Se–C stretching coordinates, respectively, the nonbonding Fe–C interactions, and the torsions and bends of the terminal ligands. This leads to the force field

$$2V = \sum_{i=1}^{4} K^{b1}(\Delta r_i^{b1})^2 + \sum_{i=1}^{8} K^{b2}(\Delta r_i^{b2})^2 + \sum_{i=1}^{4} K^{t}(\Delta r_i^{t})^2 + \sum_{i=1}^{4} K^{YC}(\Delta r_i^{YC})^2 + \sum_{k=1}^{12} H_\alpha(r_{\alpha k}\Delta\alpha_k)^2 + \sum_{k=1}^{12} H_\beta(r_{\beta k}\Delta\beta_{\beta k})^2 + \sum_{k=1}^{12} H_\gamma(r_{\gamma k}\Delta\gamma_k)^2 + \sum_{k=1}^{4} H_\delta(r_{\delta k}\Delta\delta_k)^2 + \sum_{k=1}^{4} T(\Delta\tau_k)^2 + \sum_{n=1}^{2} F_{axy}(\Delta a_n^{xy})^2 + \sum_{n=1}^{4} F_{az}(\Delta a_n^{z})^2 + \sum_{n=1}^{2} F_{bxy}(\Delta b_n^{xy})^2 + \sum_{n=1}^{4} F_{bz}(\Delta b_n^{z})^2 + \sum_{n=1}^{8} F_{cxy}(\Delta c_n^{xy})^2 + \sum_{n=1}^{4} F_{cz}(\Delta c_n^{z})^2 + \sum_{n=1}^{4} F_d(\Delta d_n)^2 + 2\sum_{n=1}^{2} F'_{axy}a_n^{xy}(\Delta a_n^{xy}) + 2\sum_{n=1}^{4} F'_{az}a_n^{z}(\Delta a_n^{z}) + 2\sum_{n=1}^{2} F'_{bxy}b_n^{xy}(\Delta b_n^{xy}) + 2\sum_{n=1}^{4} F'_{bz}b_n^{z}(\Delta b_n^{z}) + 2\sum_{n=1}^{8} F'_{cxy}c_n^{xy}(\Delta c_n^{xy}) + 2\sum_{n=1}^{4} F'_{cz}c_n^{z}(\Delta c_n^{z}) + 2\sum_{n=1}^{4} F'_{d}d_n(\Delta d_n) \quad (3)$$

where K^{b1}, K^{b2}, K^t, and K^{YC} denote the force constants of

Table 3. Approximate Force Fields of Clusters **1**−**4** (See Text) in the UBFF (3)[a,b]

	composition	K^{b1}	K^{b2}	K^{t}	K^{Y-C}[c]	$r_\alpha^2H_\alpha$	$r_\beta^2H_\beta$	$r_\gamma^2H_\gamma$	$r_\delta^2H_\delta$	F_{az}	F_{axy}	F_{bz}	F_{bxy}	F_{cz}	F_{cxy}	F_d
1	($Fe_4S^b_4S^t_4$)	1.063	0.978	1.285	2.820	0.0	0.0	0.420	0.330	0.116	0.120	0.260	0.220	0.064	0.050	0.060
2	($Fe_4Se^b_4S^t_4$)	0.758	0.856	1.277	2.820	0.0	0.0	0.420	0.330	0.094	0.120	0.222	0.208	0.076	0.054	0.060
3	($Fe_4S^b_4Se^t_4$)	1.036	0.993	1.129	2.400	0.0	0.0	0.420	0.330	0.114	0.120	0.268	0.236	0.067	0.050	0.060
4	($Fe_4Se^b_4Se^t_4$)	0.771	0.877	1.150	2.400	0.0	0.0	0.420	0.330	0.096	0.120	0.230	0.222	0.073	0.050	0.060

[a] K^i and F_i in mdyn·Å^{-1}; $r_i^2H_i$ in mdyn·Å. [b] For the force constant of the torsion T, a value of 0.03 mdyn·Å was applied. [c] The force constants for the Y−C stretches were adapted to the frequencies 690 cm^{-1} (S−C) and 571 cm^{-1} (Se−C), applying a point mass of 15 amu for the CH_3 groups.

Table 4. Force Constants for the Benzyl Cube and for Clusters **1**−**4** in the UBFF (3)[a,b]

		K^{b1}	K^{b2}	K^{t}	K^{YC}[d]	$r_\alpha^2H_\alpha$	$r_\beta^2H_\beta$	$r_\gamma^2H_\gamma$	$r_\delta^2H_\delta$	F_{az}	F_{axy}	F_{bz}	F_{bxy}	F_{cz}	F_{cx}	F_d
BC[c]	($Fe_4S^b_4S^t_4$)	1.130	0.950	1.400		0.0	0.170	0.250		0.084	0.100	0.190	0.230	0.050	0.042	
1	($Fe_4S^b_4S^t_4$)	1.063	0.978	1.285	2.820	0.0	0.0	0.420	0.330	0.116	0.120	0.260	0.220	0.064	0.050	0.060
2	($Fe_4Se^b_4S^t_4$)	0.793	0.898	1.270	2.820	0.0	0.0	0.430	0.330	0.048	0.060	0.242	0.228	0.076	0.054	0.060
3	($Fe_4S^b_4Se^t_4$)	1.000	0.940	1.230	2.400	0.0	0.180	0.440	0.330	0.094	0.100	0.160	0.138	0.077	0.055	0.060
4	($Fe_4Se^b_4Se^t_4$)	0.806	0.917	1.050	2.400	0.0	0.0	0.420	0.330	0.096	0.120	0.230	0.222	0.073	0.050	0.060

[a] K^i and F_i in mdyn·Å^{-1}; $r_i^2H_i$ in mdyn·Å. [b] For the force constant of the torsion T, a value of 0.03 mdyn·Å was applied. [c] Force constants of the benzyl cube, from ref 9. [d] The force constants for the Y−C stretches were adapted to the freqencies of 690 cm^{-1} (S−C) and 571 cm^{-1} (Se−C), applying a point mass of 15 amu for the CH_3 groups.

the bridging (b1 and b2) and terminal (t) Fe−S/Se-bonds and the Y−C bonds (Y = S, Se), respectively; H_α, H_β, H_γ, and H_δ are the bending force constants of the respective bond angles (cf. Figure 3), T represents the force constant of the torsion, and F_{axy}, F_{az}, F_{bxy}, F_{bz}, F_{cxy}, F_{cz}, and F_d are the force constants of geminal nonbonding interactions. The force constants F' appearing in the linear terms of the force field were chosen as $F'_i = (-1/10)F_i$, in agreement with the literature.[15]

On the basis of the force field (eq 3), the Fe−S force constants of the benzyl cluster, and the structural information given in Table 2, the force constants of $Fe_4S^b_4S^t_4$ cluster **1** were evaluated. To obtain a first guess of the nonbonding interactions, a q^{-9} dependence was assumed. For an estimate of the bending force constants, the respective values from the benzyl cluster were adopted. In the subsequent normal coordinate analysis, the force field of **1** was varied until optimal agreement between measured and calculated frequencies was reached. This force field is the basis for the normal coordinate analyses of the selenium substituted clusters **2**−**4**. Approximate values for the bending force constants were now adopted from $Fe_4S^b_4S^t_4$ cluster **1**. The Fe−Fe, S−S, S−Se, and Se−Se nonbonding interactions were scaled on the basis of their values in **1**, assuming a q^{-9} dependence. The unknown Fe−Se force constants K^b_{FeSe} and K^t_{FeSe} were evaluated in a first approximation from the experimentally determined Fe−S force constants K^b_{FeS} and K^t_{FeS} of **1**, employing the empirical relations

$$K^{b,t}_{FeS} = \left(\frac{A^{b,t}_{FeS} - D_{FeS}}{r^{b,t}_{FeS} - D_{FeS}}\right)^3 \quad (4)$$

and

$$K^{b,t}_{FeSe} = \left(\frac{A^{b,t}_{FeSe} - D_{FeSe}}{r^{b,t}_{FeSe} - D_{FeSe}}\right)^3 \quad (5)$$

Here, $r^{b,t}_{FeS}$ and $r^{b,t}_{FeSe}$ denote the respective Fe−S/Se-bond distances (b = bridging, t = terminal), D is a distance of closest approach, and $A^{b,t}_{FeS}$ and $A^{b,t}_{FeSe}$, respectively, are Fe−S/Se standard bond lengths which are separately defined for b and t.[16a] The constants A and D are tabulated for diatomic molecules (denoted here A^*, D^*). For the D-constants of the terminal and bridging Fe−S/Se-bonds, the respective D^* values of diatomic molecules were adopted. The b/t Fe−S standard bond lengths $A^{b,t}_{FeS}$ were determined for $Fe_4S^b_4S^t_4$ cluster **1** via eq 4, using the known Fe−S distances (Table 2), the experimentally determined force constants $K^{b,t}_{FeS}$, and the constants D^*_{FeS}. Then, the corresponding Fe−Se-standard bond lengths $A^{b,t}_{FeSe}$ were determined from the relationship

$$\frac{A^b_{FeS}}{A^b_{FeSe}} = \frac{A^t_{FeS}}{A^t_{FeSe}} = \frac{A^*_{FeS}}{A^*_{FeSe}} = \frac{2.52}{2.58} \quad (6)$$

On the basis of these $A^{b,t}_{FeSe}$ values, the known bond lengths $r^{b,t}_{FeSe}$ (Table 2), and the D values from diatomic molecules, $D^b_{FeSe} = D^t_{FeSe} = D^*_{FeSe}$, the Fe−Se force constants K^b_{FeSe} and K^t_{FeSe} could be obtained through eq 5. The approximate force fields based on these considerations are given in Table 3. As the D_{2d} distortion corresponds to two different bond lengths r^{b1} and r^{b2}, the two different force constants K^{b1}_{FeSe} and K^{b2}_{FeSe} result in a ratio which was fixed according to Badger's rule[16b,c]

$$\frac{K^{b1}_{FeSe}}{K^{b2}_{FeSe}} = \left(\frac{r^{b2}_{FeSe} - D_{FeSe}}{r^{b1}_{FeSe} - D_{FeSe}}\right)^3 \quad (7)$$

The same applies to the corresponding Fe−S force constants K^{b1}_{FeS} and K^{b2}_{FeS}.

The approximate force fields of Table 3 were then used in a fitting procedure. Results of the normal coordinate analysis of **1**−**4** are collected in Table 4 (force constants) and Table 5 (frequencies), along with the data of the benzyl cube upon which this treatment is based. A comparison between measured and calculated frequencies (Table 5) gives an impression of the good quality of the theoretical descrip-

(15) Woodward, L. A. *Introduction to the Theory of Molecular Vibrations and Vibrational Spectroscopy*; Oxford University Press: Ely House, London, 1972.

Table 5. Observed and Calculated Frequencies of the Benzyl Cube and for Clusters **1**−**4** in cm^{-1}

T_d:	A_1^t	T_2^t		T_2^b		A_1^b	E^b		T_1^b		T_2^b		
D_{2d}:	A_1^t	B_2^t	E^t	B_2^b	E^b	A_1^b	A_1^b	B_1^b	A_2^b	E^b	B_2^b	E^b	
	I	IIa	IIb	IIIa	IIIb	IV	Va	Vb	VIa	VIb	VIIa	VIIb	
BC[a]	391	367	359	385	385	335	298	283	283	270	249	243	obsd
	391	366	360	383	386	335	291	280	285	274	248	242	calcd
1	384	355	355	388	384	333	299	284	272	284	260	249	obsd
	388	355	358	388	383	333	294	285	277	285	256	252	calcd
2	370	358	347	275/286[b]	286/295[b]	218	235	235	235	223[c]	185	185	obsd
	367	357	353	277	284	216	241	238	227	229	187	186	calcd
3	297	309	309	386	378	357	289	274	274	274	239	225/219	obsd
	299	308	310	382	379	357	285	278	274	280	225	221	calcd
4	305	260	277	296	291	205	235	235	235	220	156	156	obsd
	306	259	274	299	289	206	238	238	228	227	160	156	calcd

[a] Observed and calculated frequencies for the benzyl cube, from ref 9. [b] For IIIa and IIIb, no definitive assignment is possible. [c] The band at 223 cm^{-1} is observable upon irradiation with $\lambda_{exc} = 647.1$ nm.

tion. Importantly, the Fe−S and Fe−Se force constants obtained after fitting (Table 4) are quite similar to the values derived in the empirical conversion procedure (Table 3), indicating that the first guess is already very good. Moreover, the Fe−S force constants only slightly decrease upon replacement of sulfur by selenium, concomitant with the slight increase in Fe−X bond lengths (X = S, Se). This indicates that the Fe−S and Fe−Se interactions are quite similar. The drastic spectroscopic changes occurring upon substitution of sulfur by selenium can therefore primarily be attributed to the respective mass changes. Thus, upon selective replacement of the bridging sulfur atoms by selenium, the frequencies of b modes III to VII are lowered while those of the t modes are nearly unchanged (Figure 4, A → B). Conversely, upon exclusive replacement of the terminal S by Se atoms, the t modes I and II are shifted to lower frequencies while the b modes almost remain stationary (Figure 4, A → C). Upon double S → Se substitution, finally, a shift of all modes to lower energy occurs (Figure 4, A → D). It therefore can be stated that the force field (eq 3) allows a consistent understanding of the spectra of **1**−**4**, taking into account the different masses of S and Se and the slightly different force constants of their interactions with iron.

IV. Discussion

The present study describes the application of IR and Raman spectroscopy to a series of structurally characterized Fe−S and Fe−Se cubane clusters containing all four combinations of the general composition $[Fe_4X_4(Y-CH_3)_4]^{2-}$ (X = S/Se, Y = S/Se). For maximum comparability, identical alkyl residues (CH_3) and counterions (tetrabutylammonium, TBA) have been chosen. The terminally thiolate-coordinated clusters were prepared using literature procedures. For the synthesis of terminally selenolate-coordinated clusters **3** and **4**, a new and generally applicable synthetic route has been developed. Specifically, the easily accessible halide clusters $[FeX_4Hal_4]^{2-}$ (X = S, Se; Hal = Cl, Br)[13] were reacted in a one-pot synthesis with the corresponding diselenide (R−Se−Se−R) in the presence of tetra-*n*-butylammonium borohydride [(*n*-Bu_4N)(BH_4)] and triethylamine. This leads to substitution of the terminal halide ligands by selenolate which is formed in situ by reductive cleavage of the diselenide. Single crystals suitable for X-ray structure determination could be obtained by employing recrystallization from acetonitrile (**1**) and DMSO/methanol (**2**, **3**, and **4**), respectively. All compounds are isotypic, crystallizing in the orthorhombic space group *Pba*2 with $Z = 2$ molecules in the unit cell. This offers the unique opportunity to study the structural and electronic properties of the various cluster centers in an almost identical matrix. Selenolate coordinated Fe_4S_4 and Fe_4Se_4 clusters were known, but to our knowledge have not been structurally characterized, rendering the structures of the two selenolate coordinated compounds **3** and **4** the first of such systems.

On the basis of the X-ray structural information, an interesting structural correlation between the four systems has been found. All Fe_4X_4 compounds (X = S, Se) exhibit a D_{2d} distortion of the cluster core, with the Fe_4 tetrahedron compressed along the *z*-axis and the X_4 tetrahedron elongated in this direction. In the case of the selenoclusters **2** and **4**, the elongation of the X_4 tetrahedron is larger than the compression of the Fe_4 tetrahedron, and an elongated cluster core results. In case of the sulfur clusters **1** and **3**, the opposite holds, and the cluster core is compressed (Scheme 1). Importantly, the terminal CH_3 groups are always oriented along the *z*-axis, allowing the p lone pairs of the Y donor atoms to interact with the *xy* in-plane molecular orbitals of the corresponding Fe_2X_2 diamond unit (Figure 5). This special configuration probably is the major origin for the deviation of the core geometry from ideal tetrahedral symmetry, because in solution where the terminal Y−R groups can rotate freely, cubic symmetry is observed.[9] Electron donation by the Y lone pair into the in-plane iron d-orbitals leads to an elongation of the Fe−X bonds in the *xy*-plane. This causes an increase of the Fe−Fe distance in the *xy*-plane which is the origin for the axially compressed Fe_4 geometry. Because of the larger Fe−Se bond length, this effect is less pronounced in the seleno clusters than in the sulfur clusters (cf. Scheme 1). To increase π donation of the Y lone pair into the Fe_2X_2 diamond unit, the Y−CH_3 groups are rotated into the *xy*-plane, and as a consequence the axial Fe-X bonds (along *z*) are rotated toward the *z*-axis, giving rise to the axially elongated X_4 tetrahedron. Obviously,

(16) (a) Hershbach, D. R.; Laurie, V. W. *J. Chem. Phys.* **1961**, *35*, 458−463. (b) Badger, R. M. *J. Chem. Phys.* **1934**, *2*, 128−131. (c) Badger, R. M. *J. Chem. Phys.* **1935**, *3*, 710−714.

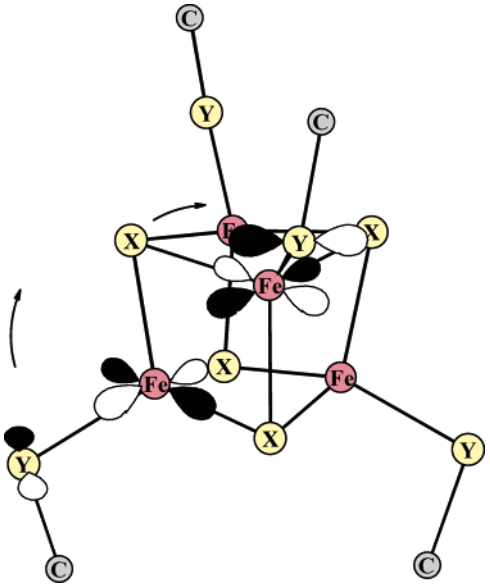

Figure 5. Interaction of the S/Se lone pairs with the Fe orbitals in the *xy*-plane (depicted schematically for two Fe irons). Arrows denote the distortion of the terminal methyl groups and the S/Se atoms in the cluster core.

this second effect is more pronounced in the case of X = Se than in the case of X = S (Scheme 1).

As known from the literature, vibrational spectroscopy, in particular Raman, can be employed to draw detailed conclusions with respect to the cluster geometry and its dependence on the terminal ligands and the crystalline environment.[17] The present investigation provides another demonstration of this approach. In combination with IR spectroscopy, the Raman spectra of all four compounds could be interpreted fully and consistently, employing a single force field which has been derived from a normal coordinate analysis of the benzyl cube.[9] By converting the Fe−S force constants with a Badger's rule relationship to Fe−Se force constants, approximate force fields for the selenium substituted clusters have been generated which were found to account for the spectral data quite well. As these Fe−Se force constants are not very different from those of their Fe−S counterparts, the striking band shifts which are apparent in the spectra are mainly due to the mass changes occurring upon substitution of terminal and bridging S atoms by Se, respectively. The use of the S → Se substitution for the evaluation of empirical force fields which has been questioned before (vide supra) thus has been demonstrated.

The finding of almost equal Fe−S and Fe−Se stretching force constants reflects very similar bonding situations in both cases. As indicated by a comparison of ionization potentials (S, 10.36 eV; Se, 9.75 eV),[18] the valence orbitals of Se are at somewhat higher energy than those of S. The electronic−structural consequences of this difference can most simply be studied in tetrahedral $[Fe(XMe)_4]^{2-}$ complexes (X = S, Se; cf. Supporting Information). The spin-up and spin-down level schemes of both systems are greatly split by spin-polarization, and both exhibit bands of Fe−X (antibonding), Fe−X (bonding), and X (nonbonding) orbitals which are at comparable energies for $[Fe(SMe)_4]^{2-}$ and $[Fe(SeMe)_4]^{2-}$. An important difference between both systems is the fact that the highest occupied minor spin-orbital has primarily d-character in the case of $[Fe(SMe)_4]^{2-}$ and primarily ligand (Se) character in the case of $[Fe(SeMe)_4]^{2-}$, reflecting the higher energy of the Se 4p orbitals in comparison to S 3p. Overall, however, Fe−X covalency (X = S, Se) is found to be very similar in both complexes; i.e., the potential loss of metal−ligand overlap upon going from Fe−S to Fe−Se because of the increase in the Fe−X bond length (∼0.10−0.17 Å, cf. Table 2) is obviously compensated by more diffuse p orbitals of Se as compared to S. Therefore, no big differences in metal−ligand force constants are expected upon substitution of sulfur by selenium, in agreement with the vibrational spectroscopic results of this study. In the accompanying paper, the employed force field is modified to account for the vibrational spectra of molybdenum substituted iron−sulfur clusters which are of relevance to the enzyme nitrogenase.

Acknowledgment. F.T. thanks the State of Schleswig-Holstein and FCI for funding of this research. A.K. acknowledges the help of Natascha Böres with preparative work and of Uschi Cornelissen with the spectroscopic measurements.

Supporting Information Available: CIF files of the four structures which are also deposited with the Cambridge Crystallographic Data Centre (CCDC-217545 (**1**), CCDC-201199 (**2**), CCDC-201200 (**3**), and CCDC-201198 (**4**)) and DFT calculations of $[Fe(SMe)_4]^{2-}$ and $[Fe(SeMe)_4]^{2-}$. This material is available free of charge via the Internet at http://pubs.acs.org.

IC030347D

(17) Maes, E. M.; Knapp, M. J.; Czernuszewicz, R. S.; Hendrickson, D. N. *J. Phys. Chem. B* **2000**, *104*, 10878−10884.
(18) Moore, C. E. *Ionization Potentials and Ionization Limits Derived from the Analysis of Optical Spectra*; NSRDS-NBS 34; U.S. Government Printing Office: Washington, DC, 1970.